Formation process of mixed fouling of microbe and CaCO$_3$ in water systems*

Tianqing Liu*, Xiangqin Li, Hongling Wang, Xiangyu Sun

Chemical Engineering Research Institute, Dalian University of Technology, Dalian 116012, China

Abstract

The mixed fouling process of *Pseudomonas fluorescens* and CaCO$_3$ on different solid surfaces in a simulated cooling water system has been investigated. The mixed fouling behavior on different solid surfaces under the condition of different CaCO$_3$ saturation levels and bulk velocities has been examined, and the growth curves of mixed fouling have been obtained. The results show that the mixed fouling behavior on various material surfaces depends mainly on the affinity of bacteria to a material. The mixed fouling mass developed on polymer materials is much more than that on metal surfaces. With the increase of saturation level of CaCO$_3$, however, this difference becomes minimal. The results also indicate that the mixed fouling mass decreases with the increase of CaCO$_3$ saturation degree and velocity. The induction period of mixed fouling declines with the rising of velocity. Moreover, the induction period of mixed fouling is longer than that of pure biofouling when the saturation level of CaCO$_3$ is less than 1 and greater than 0. The induction period decreases with CaCO$_3$ saturation degree when the level is more than or equal to 1.

In addition, the sequence of adhesion and deposit of the bacteria and CaCO$_3$ on a glass surface was measured with micro-video technology. The results show that CaCO$_3$ first deposits on the solid surface, while the bacteria need longer time to adhere on the surface.
© 2002 Elsevier Science B.V. All rights reserved.

Keywords: Bacteria; Calcium carbonate; Mixed fouling; Induction period; Materials

1. Introduction

Mixed fouling of microorganism and other minerals existing in various water systems takes place when the water flows through equipment and pipes [1]. It may decrease the performance of equipment, increase pressure drop in water circuits, introduce thermal resistance in heat exchangers, pollute water and products, and induce corrosion of surface materials. Another kind of harmful mixed fouling made of bacteria and minerals may take place on the surfaces of catheters and stents [2] which are applied in the urinary system of the human body as well as on the teeth [3]; this can induce urolithiasis or periodontitis.

Although much research about fouling has been carried out [4–6], almost all the studies were aimed at a single kind of fouling, such as biofouling, crystallization fouling or particular fouling. Most of the fouling developed in industrial processes, however, is a mixed one. The mixed fouling

consisting of microbes and calcium or magnesium salts is, in particular, the major part of the fouling in real water systems. Therefore it will accord more with real processes to investigate the mixed fouling formed with micro-organism and calcium or magnesium deposits. Also the investigation is essential to understand the interaction between bacteria and minerals, the mechanism and the sequence of the mixed fouling, and to develop novel techniques for controlling the mixed fouling.

The process of mixed fouling with *Pseudomonas fluorescens* and CaCO$_3$ developed on different solid surfaces in simulated cooling water system is investigated in this paper. The influences of velocity and saturation level of CaCO$_3$ on the mixed fouling mass and the induction period have been experimentally determined. Meanwhile, the formation process and the sequence of mixed fouling have been revealed by means of micro-video technology.

2. Experiment

The experimental apparatus is shown in Fig. 1. The fermenter with 3.3 l in volume was used for a monoculture of

* Corresponding author. Tel.: +86-411-363-1333-3239;
fax: +86-411-363-3080.
E-mail address: liutq@dlut.edu.cn (T. Liu).

Nomenclature

e	average surface roughness (μm)
F	average mixed fouling mass (mg/cm^2)
K	concentration product of Ca^{2+} and CO$_3^{2-}$ ions in water (mol/l)^2
K_{sp}	solubility product of CaCO$_3$ in water (mol/l)^2
t_f	induction period of mixed fouling (h)

P. fluorescens, which is commonly found in water systems. Medium or nutrients and air were fed into the fermenter to maintain a constant cell concentration in it. Alkali (2 M potassium hydroxide) was automatically added in order to maintain a constant pH value. The composition of medium used is given in Table 1 and the operating conditions of the fermenter are given in Table 2.

A mixing vessel with 10 l capacity was used to provide simulated water containing a certain concentration of the bacteria. There are five streams fed into the vessel, including streams from:

1. the fermenter to provide the contaminating bacteria;
2. the nutrient supply reservoir;
3. the filtered water to provide make up water;
4. Na$_2$CO$_3$ aqueous solution;
5. CaCl$_2$ aqueous solution.

The simulated water was pumped through two test sections and returned to the mixing vessel. The operating conditions of circulating water system are shown in Table 3. Here, the saturation level of CaCO$_3$ is defined as K/K_{sp}, namely the ratio of the concentration product of Ca^{2+} ion

Table 1
The composition of medium and microelement solution

Composition	Concentration (g/l)
(a) The composition of medium	
NaH$_2$PO$_4$	0.775
Na$_2$HPO$_4$	5.5
K$_2$SO$_4$	1.75
MgSO$_4\cdot$7H$_2$O	0.1
Na$_2$EDTA$\cdot$2H$_2$O	0.8303
NH$_4$Cl	3.82
Microelement	1 ml
Glucose	5.0
(b) The composition of microelement solution	
MnSO$_4\cdot$4H$_2$O	13.00
H$_3$BO$_3$	3.00
ZnSO$_4\cdot$7H$_2$O	2.00
Na$_2$MoO$_4\cdot$H$_2$O	0.25
CuSO$_4\cdot$5H$_2$O	0.025
CoCl$_2\cdot$6H$_2$O	0.024

Table 2
The operation conditions in fermenter

Medium flow rate (ml/h)	66
Air flow rate (l/min)	5.5
Bacteria concentration (cells/ml)	1×10^9
Temperature (°C)	22–27
pH	6.5–7.0

and CO$_3^{2-}$ ion in water to the solubility product of CaCO$_3$. By regulating the concentration of CaCl$_2$ and Na$_2$CO$_3$ solution and controlling their flow rates into the circulating water system, the saturation degree of CaCO$_3$ in water can be adjusted within 0–10. The concentration of CO$_3^{2-}$ was
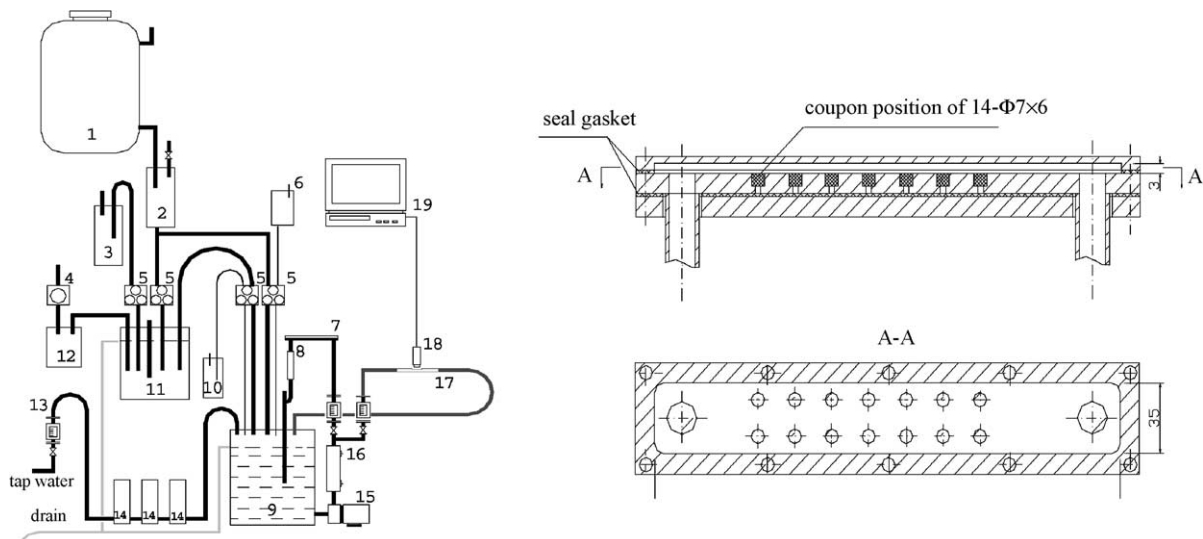

Fig. 1. Experimental apparatus and test section: 1, medium container; 2, interim container; 3, alkali aqueous container; 4, air compressor; 5, peristaltic pump; 6, Na$_2$CO$_3$ solution tank; 7, test section (a); 8, cooling section; 9, mixing trough; 10, CaCl$_2$ solution tank; 11, fermenter; 12, humidifier; 13, flowmeter; 14, filter; 15, magnetic pump; 16, heater; 17, test section (b); 18, micro-video camera; 19, monitor.

Table 3
The operation conditions of circulating water system

Medium flow rate (ml/h)	66
Bacteria flow rate (ml/h)	30
Bacteria concentration (cells/ml)	1×10^6
Velocities in test section (a) (m/s)	0.8, 1.0, 1.2
Velocities in test section (b) (m/s)	0.4, 0.76
Three-stage filtered water flow rate (l/h)	11.36
$CaCl_2$ solution flow rate (ml/min)	0.5
Na_2CO_3 solution flow rate (ml/min)	0.5
Saturation levels of $CaCO_3$	0, 0.64, 1, 10
Temperature (°C)	35

determined according to the equilibrium equations of CO_3^{2-} and HCO_3^- as well as the amount of Na_2CO_3 added and pH value. The bacteria content in circulated water was measured with plate cell counter and it was controlled at 1×10^6 cells/ml.

The test section (a) shown in Fig. 1 is a rectangular flow path with 400 mm in length, 40 mm in width, and 3 mm in height. It is made of plexiglass. On the bottom of the flow path there are fourteen 7 mm holes used to inlay coupons which were 7 mm in diameter and 6 mm in height. The distance from the entrance of fluid to the test surface of the coupons is more than 250 mm so that the influence of entrance can be ignored. The weight of mixed fouling formed on the surfaces of coupons was measured with an analytical balance with 0.1 mg accuracy.

Test section (b) is made of a plexiglass pipe with 7 mm in inner diameter and 250 mm in length. A $25 \times 3 \, mm^2$ rectangular slot was manufactured along the axis of the pipe in the middle of it. A piece of plain glass with 0.2 mm in thickness was sealed on the slot. Then the test section was fixed under the XSZ-CTV micro-video system so that the dynamic process of mixed fouling formation on the glass surface can be viewed and recorded.

The flow system was first washed with ClO_2 solution after each run of the test until there was no mixed fouling within the system. Then fresh filtered water was used to wash the loop at least four times.

3. Experimental results and discussions

3.1. Growth curves of mixed fouling

The dynamic formation process of mixed fouling of bacteria and $CaCO_3$ was measured for 10 kinds of solid materials under the conditions of three different velocities and four levels of $CaCO_3$ saturation. The growth curves of mixed fouling under these varied conditions have been obtained. Fig. 2 only shows the results on the surfaces of copper and stainless steel as typical examples. It can be seen from the figure that all of the formation processes experience a certain initial period called induction period [7] before mixed fouling increases clearly. Besides, the area of flow

section will become smaller and smaller as the mixed fouling mass increases. Under the condition of constant flow rate, the real velocity over the fouling layer will rise and so does the shear stress. Partial fouling layer will peel off when the attraction between the substances within fouling layer is less than the shear stress [8]. After this, the process of growth and drop occurs irregularly, which produces the growth curves of mixed fouling in a state of irregular sawtooth.

It is also clear from Fig. 2 that the changes of velocity and $CaCO_3$ saturation level have obvious influence on the growth curves of the mixed fouling. As velocity rises, i.e. when the shear stress increases, the mixed fouling is suppressed. Therefore the curves' positions become lower and the average fouling mass reduces. Additionally, as the $CaCO_3$ saturation degree increases, the fluctuation extent of the growth curves decreases and the average mixed fouling mass also declines. This results from the following factors. Firstly, the activity of bacteria in water is inhibited and their adhesion to solid surface reduces as the ion concentration of Ca^{2+} rises. Secondly, the $CaCO_3$ deposit becomes the more important component in the mixed fouling layer in this case, but its dropping amount is far less than that of bacteria biofouling. Thirdly, the coupons was not heated in this experiment, so, $CaCO_3$ deposit did not increase rapidly. All these make the mixed fouling mass decrease with the increase of $CaCO_3$ saturation level.

3.2. Mixed fouling mass and induction period

The original data of all growth curves were analyzed and processed in order to express and compare clearly the induction period and average mass of mixed fouling formed on different material surfaces under various velocities and $CaCO_3$ saturation levels. The results are shown in Fig. 3. Here, the mixed fouling induction period comes from the initial time period of each growth curve before the mixed fouling mass rises obviously. The average mixed fouling mass means the average weight of mixed fouling per unit area of the material surface.

From Fig. 3 the effects of material, velocity and $CaCO_3$ saturation level on the average fouling mass and induction period can be clearly figured out, which is illustrated as follows.

The influence of velocity: both the mixed fouling mass and induction period on various materials decrease as velocity increases. This results from the action of shear stress. The dropping amount of fouling layer will increase with shear stress, which limits the further development of the mixed fouling mass. For the induction period, the increase of velocity will result in a higher mass transfer rate of $CaCO_3$ towards solid surface. At the same time, the migration and adhesion of the bacteria in water onto the surfaces are enhanced for the bacteria to avoid the increased shear stress when velocity rises. Therefore, the induction period of mixed fouling becomes shorter.
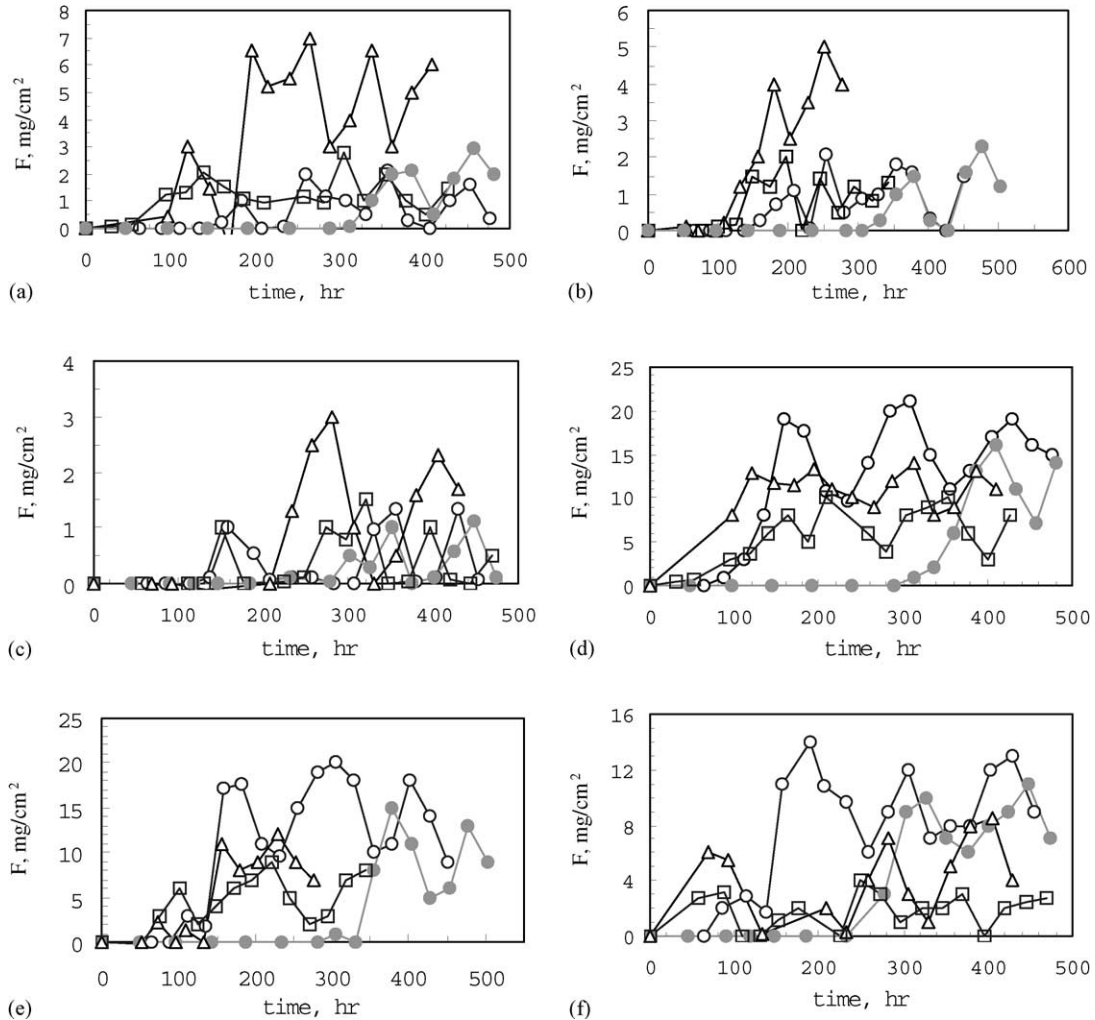
Fig. 2. Growth curves of the mixed fouling on copper and stainless steel: (a) copper, 0.8 m/s; (b) copper, 1 m/s; (c) copper, 1.2 m/s; (d) stainless steel, 0.8 m/s; (e) stainless steel, 1 m/s; (f) stainless steel, 1.2 m/s. (○) Saturation level 0; (●) saturation level 0.64; (△) saturation level 1; (□) saturation level 10.

The influence of $CaCO_3$ saturation level: for the mixed fouling mass, it decreases with the increase of $CaCO_3$ saturation level. This is because the bacteria biofouling is the controlled component in mixed fouling when the solid surface is not heated. The activity of bacteria as well as the ability of their adhesion and secreting slim are suppressed when the saturation degree of $CaCO_3$ gets higher. As a result, the mixed fouling mass reduces.

For the induction period, since there is little $CaCO_3$ deposits when the saturation level of $CaCO_3$ is less than 1 and greater than 0, the induction period in this situation depends only on the adhesion of bacteria. The induction period at this time is longer than that of pure biofouling because the activity of bacteria in this case is lower than that when there is no Ca^{2+} in water. However, $CaCO_3$ will deposit onto the solid surface and end the induction period when the saturation level of $CaCO_3$ is more than or equal to 1, although the activity of bacteria is still limited. In this case, the induction period becomes shorter as the $CaCO_3$ saturation level rises.

3.3. Process and sequence of mixed fouling formation

The dynamic process of the mixed fouling formed with the bacteria and $CaCO_3$ was investigated in test section (b) by means of the micro-video technology. Fig. 4 shows some typical results, which indicate that $CaCO_3$ particles are the first fouling component appearing on a clean solid surface, while bacteria adhere later when the saturation degree of $CaCO_3$ in water is more than or equal to 1. The reason for this sequence is that the bacteria can adhere to a solid surface only after a conditioned film [9] has formed on the surface and after they fit the new environment. $CaCO_3$, on the other hand, is inorganic material; its deposit on solid surfaces depends only on the saturation level. It is relatively easy to deposit on a surface if the saturation condition is satisfied. As a result, $CaCO_3$ particles will appear on the solid surfaces earlier than bacteria.

It was also observed during the experiment that the activity of the bacteria decreases and the bacteria could be buried as
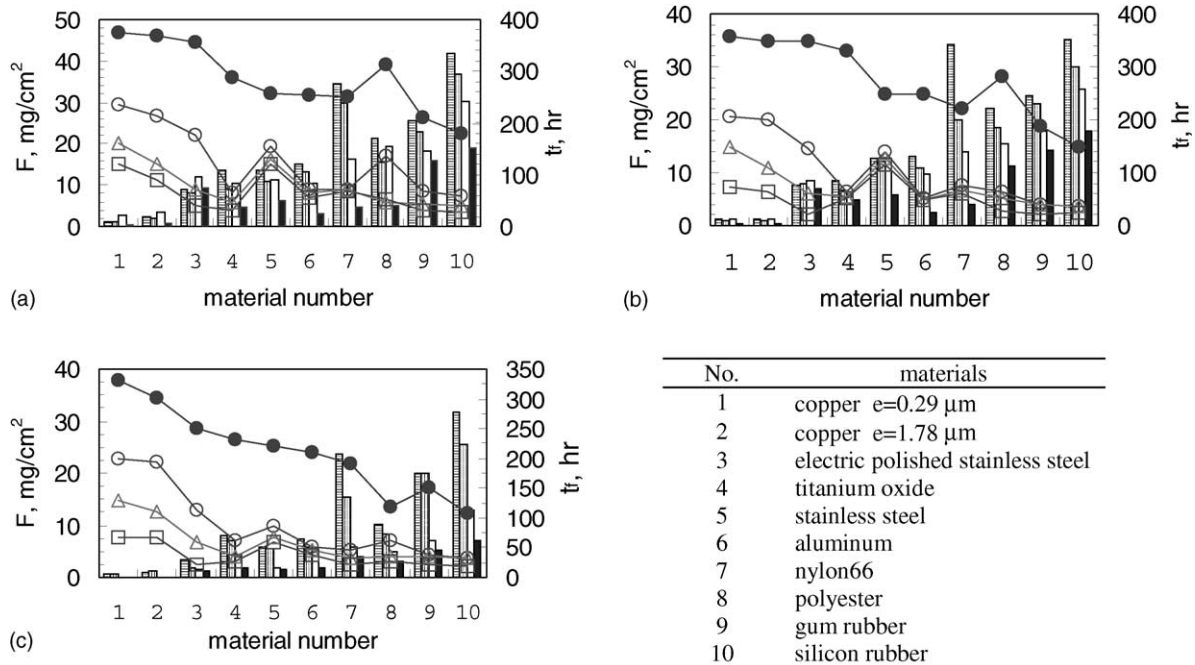
Fig. 3. Average mixed fouling mass and induction period on different materials: (a) 0.8 m/s; (b) 1 m/s; (c) 1.2 m/s. (▭) Mixed fouling, saturation level 0; (▥) mixed fouling, saturation level 0.64; (□) mixed fouling, saturation level 1; (■) mixed fouling, saturation level 10; (○) induction period, saturation level 0; (●) induction period, saturation level 0.64; (△) induction period, saturation level 1; (□) induction period, saturation level 10.

the mixed fouling developed. The bacteria buried by CaCO$_3$ deposits may become dormant or die because of the shortage of nutrients. The mixed fouling was thus formed with the bacteria and their extracellular matrix as well as CaCO$_3$ particles mixed together, as shown in Fig. 4d. There were bacteria and CaCO$_3$ at each layer inside the mixed fouling and the active bacteria usually appear at the interface between water phase and mixed fouling surface. The mixed fouling grows relatively fast during the initial period of the process, which mainly results from the effect of CaCO$_3$ deposits. After the induction period, the thickness of the mixed fouling layer starts to fluctuate, but within 300–500 μm.
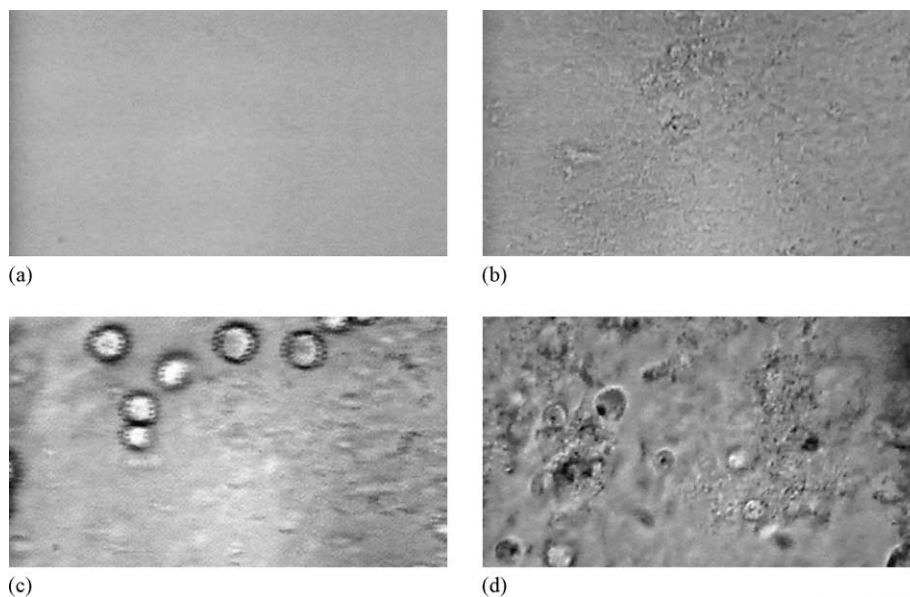

Fig. 4. The formation sequence and structure of mixed fouling, 0.4 m/s, saturation level = 1: (a) original surface (×3600); (b) CaCO$_3$ deposits firstly (×3600); (c) bacteria adhere later (×3600); (d) the surface of mixed fouling (×3600).

4. Conclusions

The following conclusions can be obtained from the above study:

1. The mixed fouling behavior on different material surfaces depends mainly on the affinity of the bacteria to a material. The mixed fouling mass formed on polymers is obviously more than that on metals. This difference becomes smaller when the saturation level of $CaCO_3$ is high.
2. The induction period and average mass of the mixed fouling reduce as velocity rises.
3. The mixed fouling mass decreases with the increase of $CaCO_3$ saturation level. For the induction period of mixed fouling, it is longer than that of pure biofouling when the $CaCO_3$ saturation degree is less than 1 and more than 0. After the level is more than or equal to 1, however, the induction period of mixed fouling becomes shorter as the level increases.
4. During the initial formation process of the mixed fouling, $CaCO_3$ firstly deposits on a solid surface while bacteria adhere later.

References

[1] T.R. Bott, Heat exchanger cleaning, in: T.R. Bott (Ed.), Fouling of Heat Exchangers, Elsevier, Amsterdam, 1995, pp. 357–407 (Chapter 15).

[2] J. Nickel Curtis, J.C. Robert, Bacterial biofilms in urology, Infect. Urol. 11 (6) (1998) 169–175. http://www.medscape.com/scp/iiu/1998/v11.n06/u3004.nick/.

[3] T. John, Interactions of bacteria and amebas with ocular biomaterials, Cells Mater. 1 (2) (1991) 129–139.

[4] N. Epstein, Fouling in heat transfer, in: Proceedings of the Sixth International Heat Transfer Conference, Vol. 6, 1978, pp. 235–253.

[5] W.L. Van Nostrand, S.H. Leach Jr., J.L. Haluska, Economic penalties associated with the fouling of refinery heat transfer equipment, in: Somerscales, Knudsen (Eds.), Fouling of Heat Transfer Equipment, 1981, 619 pp.

[6] S. Yang, Z. Xu, Fouling and Countermeasures for Heat Transfer Equipment, Scientific Publishing House, 1995 (in Chinese).

[7] T. Liu, X. Wang, Fouling induction period of $CaCO_3$ on heated surface, Chin. J. Chem. Eng. 7 (3) (1999) 230.

[8] M.M. Pinheiro, L.F. Bott, Surface phenomena and hydrodynamic effects on the deposition of *Pseudomonas fluorescens*, Can. J. Chem. Eng. 66 (1988) 63–67.

[9] P.S. Meadows, The microbiology of interfaces in the marine environment, in: M.J. Bull (Ed.), Progress in Industrial Microbiology, Vol. 13, Elsevier, Amsterdam, 1979, pp. 207–265.